Inorganic Chemistry
Article

Inorg. Chem. **2010**, *49*, 1439–1448 **1439**
DOI: 10.1021/ic901660m

Electrochemiluminescent Functionalizable Cyclometalated Thiophene-Based Iridium(III) Complexes

Marco Bandini,* Michele Bianchi, Giovanni Valenti, Fabio Piccinelli,† Francesco Paolucci, Magda Monari, Achille Umani-Ronchi, and Massimo Marcaccio*

Dipartimento di Chimica "G. Ciamician", Alma Mater Studiorum, Università di Bologna, via Selmi 2, 40126 Bologna, Italy. † Current address: Laboratory of Solid state Chemistry -DB-University of Verona, Strada le Grazie 15, Cá Vignal 1, 37134, Verona, Italy.

Received August 19, 2009

A family of new functional bis-cyclometalated thiophene-based cationic iridium complexes have been prepared and fully characterized. The introduction of formyl groups into the thienyl-based cyclometalating ligand (thpy-CHO) allows one to perform further functionalizability and to confer to the whole species potentially interesting perspectives as functional materials. The X-ray crystal structures of three complexes, namely, $[Ir(thpy)_2bpy]PF_6$, $[Ir(thpy\text{-}CHO)_2bpy]PF_6$, and $[Ir(thpy\text{-}CHO)_2phen]PF_6$, are reported. A rich reduction voltammetric pattern of the complexes is outlined, and the effect of the substituents on the cyclic voltammetric behavior is fully elucidated. Finally, the electrochemiluminescence spectra of all of the species have been obtained in acetonitrile by annihilation of the one-electron-oxidized and -reduced forms, showing very similar features with respect to the luminescence (as both the shape and energy of the emission bands).

Introduction

After the pioneering work of Forrest, Thompson, and coworkers[1] over the past decade, many efforts have been devoted toward the design, synthesis, and photophysical investigation of new phosphorescent cyclometalated iridium(III) complexes.[2] Solution processability, thermal stability, color versatility (tuning over the whole visible range has been covered by ligand modification),[3] high external quantum efficiency (QE), and short phosphorescence lifetimes make these species valuable candidates for numerous technological applications. Among them, full-display technology and lighting are of particular relevance.[4] Depending on the nature of the organic ligands, cyclometalated iridium complexes can be divided into two groups: neutral homo- and heteroleptic complexes[5] of the general formulas $[Ir(C^\wedge N)_3]$ and $[Ir(C^\wedge N)_2(X^\wedge X)]$ (X = O, N) and charged analogues of the general formulas $[Ir(C^\wedge N)_2(N^\wedge N)]^+$ (cationic)[6] and

*To whom correspondence should be addressed. E-mail: marco.bandini@unibo.it (M.B.), massimo.marcaccio@unibo.it (M.M.).

(1) Baldo, M. A.; O'Brien, D. F.; You, Y.; Shoustikov, A.; Sibley, S.; Thompson, M. E.; Forrest, S. R. *Nature* **1998**, *395*, 151.

(2) For representative examples, see: (a) Baldo, M. A.; Lamansky, S.; Burrows, P. E.; Thompson, M. E.; Forrest, S. R. *Appl. Phys. Lett.* **1999**, *75*, 4. (b) O'Brien, D. F.; Baldo, M. A.; Thompson, M. E.; Forrest, S. R. *Appl. Phys. Lett.* **1999**, *74*, 442. (c) Baldo, M. A.; Adachi, C.; Forrest, S. R.; Thompson, M. E. *Appl. Phys. Lett.* **2000**, *77*, 904. (d) Lamansky, S.; Djurovich, P.; Murphy, D.; Abdel-Razzaq, F.; Kwong, R.; Tsyba, I.; Bortz, M.; Mui, B.; Bau, R.; Thompson, M. E. *Inorg. Chem.* **2001**, *40*, 1704. (e) Lamansky, S.; Djurovich, P.; Murphy, D.; Abdel-Razzaq, F.; Lee, H.-E.; Adachi, C.; Burrows, P. E.; Forrest, S. R.; Thompson, M. E. *J. Am. Chem. Soc.* **2001**, *123*, 4303. (f) Adachi, C.; Baldo, M. A.; Thompson, M. E.; Forrest, S. R. *J. Appl. Phys.* **2001**, *90*, 5048. (g) Holmes, R. J.; D'Andrade, B. W.; Forrest, S. R.; Ren, X.; Li, J.; Thompson, M. E. *Appl. Phys. Lett.* **2003**, *83*, 3818. (h) Coppo, P.; Plummer, E. A.; De Cola, L. *Chem. Commun.* **2004**, 1774.

(3) (a) Lowry, M. S.; Hudson, W. R.; Pascal, R. A., Jr.; Bernhard, S. *J. Am. Chem. Soc.* **2004**, *126*, 14129. (b) You, Y.; Park, S. Y. *J. Am. Chem. Soc.* **2005**, *127*, 12438 and references cited therein. (c) Avilov, I.; Minnofar, P.; Cornil, J.; De Cola, L. *J. Am. Chem. Soc.* **2007**, *129*, 8247.

(4) (a) Holder, E.; Langeveld, B. M. W.; Schubert, U. S. *Adv. Mater.* **2005**, *17*, 1109 and references cited therein. (b) Evans, R. C.; Douglas, P.; Winscom, C. J. *Coord. Chem. Rev.* **2006**, *250*, 2093. (c) Chou, P. T.; Chi, Y. *Eur. J. Inorg. Chem.* **2006**, 3319–3332. (d) Walzer, K.; Maennig, B.; Pfeiffer, M.; Leo, K. *Chem. Rev.* **2007**, *107*, 1233. (e) Chou, P.-T.; Chi, Y. *Chem.—Eur. J.* **2007**, *13*, 380–395. (f) Chou, P.-T.; Chi, Y. *Chem. Soc. Rev.* **2007**, *36*, 1421–1431.

(5) For representative examples, see: (a) Tsuboyama, A.; Iwawaki, H.; Furugori, M.; Mukaide, T.; Kamatani, J.; Igawa, S.; Moriyama, T.; Miura, S.; Takiguchi, T.; Okada, S.; Hoshino, M.; Ueno, K. *J. Am. Chem. Soc.* **2003**, *125*, 12971. (b) Okada, S.; Okinaka, K.; Iwawaki, H.; Furugori, M.; Hoshimoto, M.; Mukaide, T.; Kamatani, J.; Igawa, S.; Tsuboyama, A.; Takiguchi, T.; Ueno, K. *J. Chem. Soc., Dalton. Trans.* **2005**, 1583. (c) Dedeian, K.; Shi, J.; Sheperd, N.; Forsythe, R.; Morton, D. C. *Inorg. Chem.* **2005**, *44*, 4445. (d) Ragni, R.; Plummer, E. A.; Brunner, K.; Hofstraat, J. W.; Babudri, F.; Farinola, G. M.; Naso, F.; De Cola, L. *J. Mater. Chem.* **2006**, *16*, 1161. (e) Bolink, H. J.; Coronado, E.; Santamaria, S. G.; Sessolo, M.; Evans, N.; Klein, C.; Baranoff, E.; Kalyanasundaram, K.; Graetzel, M.; Nazeeruddin, Md. K. *Chem. Commun.* **2007**, 3276–3278. (f) Yang, C.-H.; Cheng, Y.-M.; Chi, Y.; Hsu, C.-J.; Fang, F.-C.; Wong, K.-T.; Chou, P.-T.; Chang, C.-H.; Tsai, M.-H.; Wu, C.-C. *Angew. Chem., Int. Ed.* **2007**, *46*, 2418. (g) Ragni, R.; Orselli, E.; Kottas, G. S.; Omar, O. H.; Babudri, F.; Pedone, A.; Naso, F.; Farinola, G. M.; De Cola, L. *Chem.—Eur. J.* **2008**, *15*, 136. (h) McDonald, A. R.; Lutz, M.; von Chrzanowski, L. S.; van Klink, G. P. M.; Spek, A. L.; van Koten, G. *Inorg. Chem.* **2008**, *47*, 6681.

(6) (a) Yang, C.-H.; Li, S.-W.; Chi, Y.; Cheng, Y.-M.; Yeh, Y.-S.; Chou, P.-T.; Lee, G.-H.; Wang, C.-H.; Shu, C.-F. *Inorg. Chem.* **2005**, *44*, 7770. (b) Tamayo, A. B.; Garon, S.; Sajoto, T.; Djurovich, P. I.; Tsyba, I. M.; Bau, R.; Thompson, M. E. *Inorg. Chem.* **2005**, *44*, 8723. (c) Su, H.-C.; Wu, C.-C.; Fang, F.-C.; Wong, K.-T. *Appl. Phys. Lett.* **2006**, *89*, 261118. (d) Lowry, M. S.; Bernhard, S. *Chem.—Eur. J.* **2006**, *12*, 7970 and references cited therein. (e) Zhao, Q.; Liu, S.; Shi, M.; Li, F.; Jing, H.; Yi, T.; Huang, X. *Organometallics* **2007**, *26*, 5922. (f) Volpi, G.; Garino, C.; Salassa, L.; Fiedler, J.; Hardcastle, K. I.; Gabetto, R.; Nervi, C. *Chem.—Eur. J.* **2009**, *15*, 6415.

Published on Web 01/14/2010

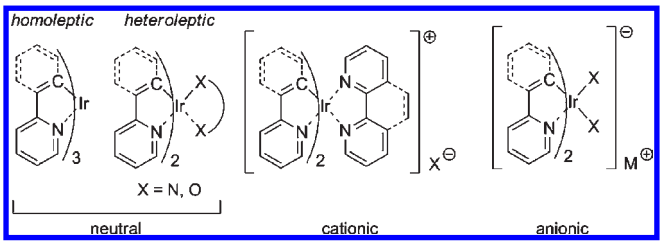

Figure 1. General structures of cyclometalated iridium(III) complexes.

$[Ir(C^N)_2X_2]^-$ (anionic).[7] The symbols C^N and N^N/O^O represent the cyclometalating and ancillary ligands, respectively, as sketched in Figure 1.

Nowadays, numerous studies account for the remarkable potentialities and attitude of the neutral iridium(III) complexes as triplet emitters for electroluminescent devices. On the contrary, ionic transition-metal complexes (iTMCs) have received less attention even though some peculiar physical/chemical properties should allow one to overcome a number of drawbacks occurring with neutral species.[8]

With particular concern for the cationic bis-cyclometalated iridium complexes, the possibility of assembling efficient single-layer nonencapsulated devices with air-stable electrodes has been envisaged. Operational simplicity combined with low turn-on voltages (usually < 3 V) led to the production of light-emitting electrochemical cells (LECs)[9] and polymerically analogous LECs[10] with fine tuning of the emission color from yellow to blue.[11] Moreover, in the search for new materials, charged iridium(III) complexes have found application as second-order nonlinear optical phosphors[12] and photosensitizers for hydrogen production.[13]

A very important and potentially appealing applicative field of charged iridium(III) cyclometalated polypyridine complexes is represented by their use in biological tagging for proteins, peptides, amino acids, antibodies, oligonucleotides, and so on.[14] This requires adequately functionalized cyclometalating or ancillary ligands to tether the biomolecules, thus obtaining luminescent labeling reagents.

Although the chemical manipulation of preformed iridium complexes has been described,[15] the use of prefunctionalized organic counterparts in the iridium-based complexes remains the widely employed approach.[16] In this context, the use of formyl groups was dictated by the chemical feasibility of further chemical manipulations and tethering.

Recently, there has been a "renaissance" of electrogenerated chemiluminescence as a powerful biodetection tool because it brings all of the potentialities of the luminescence techniques with an uncommon higher sensitivity and without the need for use of an exciting light. A comprehensive investigation on the electrochemiluminescence (ECL) of functionalized cyclometalated iridium(III) complexes has not been reported so far.[17]

Our ongoing interest in the development of unprecedented "outer-sphere" metal complexes based on oligo- and polythienyl ligands[18,19] led us to consider 2-thienylpyridine (thpy) as a basic structural motif for the cyclometalating ligands. In fact, the unique properties of thienyl compounds to undergo direct and selective chemical/electrochemical polymerization would allow the efficient incorporation of iridium phosphors into functional organic semiconductors.

In the present study, a series of cationic iridium complexes have been prepared by using different combinations of bispyridine neutral ligands (N^N) and thiophene-based substituted cyclometalating (C^N) ligands (Chart 1).[20] A thorough investigation of the structural, optical, and electrochemical properties is also reported.

Experimental Section

General Experiments. ^{1}H NMR spectra were recorded on Varian 200 (200 MHz) and Varian 300 (300 MHz) spectrometers. Chemical shifts are reported in ppm from tetramethylsilane with

(7) Nazeeruddin, M. K.; Humphry-Baker, R.; Berner, D.; Rivier, S.; Zuppiroli, L.; Graetzel, M. *J. Am. Chem. Soc.* **2003**, *125*, 8790.

(8) Lowry, M. S.; Goldsmith, J. I.; Slinker, J. D.; Rohl, R.; Pascal, R. A.; Malliaras, G. G.; Bernhard, S. *Chem. Mater.* **2005**, *17*, 5712.

(9) (a) Pei, Q.; Yu, G.; Zhang, C.; Yang, Y.; Heeger, A. J. *Science* **1995**, *269*, 1086. (b) Pei, Q.; Yang, Y.; Yu, G.; Zhang, C.; Heeger, A. J. *J. Am. Chem. Soc.* **1996**, *118*, 3922. (c) Leger, J. M. *Adv. Mater.* **2008**, *20*, 837.

(10) (a) Liu, S.-H.; Zhao, Q.; Chen, R.-F.; Deng, Y.; Fan, Q.-L.; Li, F.-Y.; Wang, L.-H.; Huang, C.-H.; Huang, W. *Chem.—Eur. J.* **2006**, *12*, 4341. (b) Du, B.; Wang, L.; Wu, H.; Yang, W.; Zhang, Y.; Liu, R.; Sun, M.; Peng, J.; Cao, Y. *Chem.—Eur. J.* **2007**, *13*, 7432.

(11) (a) Slinker, J. D.; Gorodetsky, A. A.; Lowry, M. S.; Wang, J.; Parker, S.; Rohl, R.; Bernhard, S.; Malliaras, G. G. *J. Am. Chem. Soc.* **2004**, *126*, 2763. (b) Parker, S. T.; Slinker, J. D.; Lowry, M. S.; Cox, M. P.; Bernhard, S.; Malliaras, G. G. *Adv. Mater.* **2005**, *17*, 3187. (c) Slinker, J. D.; Koh, C. Y.; Malliaras, G. G.; Lowry, M. S.; Bernhard, S. *Appl. Phys. Lett.* **2005**, *86*, 173506. (d) Nazeeruddin, Md. K.; Wegh, R. T.; Zhou, Z.; Klein, C.; Wang, Q.; De Angelis, F.; Fantacci, C.; Grätzel, M. *Inorg. Chem.* **2006**, *45*, 9245. (e) Bolink, H. J.; Cappelli, L.; Coronado, E.; Gratzel, M.; Orti, E.; Costa, R.; Viruela, P. M.; Nazeeruddin, Md. K. *J. Am. Chem. Soc.* **2006**, *128*, 14786. (f) Bolink, H. J.; Cappelli, L.; Cheylan, S.; Coronado, E. D.; Costa, R.; Lardiés, N.; Nazeeruddin, Md. K; Orti, E. *J. Mater. Chem.* **2007**, *17*, 5032. (g) De Angelis, F.; Fantacci, S.; Evans, N.; Klein, C.; Zakeeruddin, S. M.; Moser, J. E.; Kalyanasundaram, K.; Bolink, H. J.; Graetzel, M.; Nazeeruddin, Md. K. *Inorg. Chem.* **2007**, *46*, 5989.

(12) Dragonetti, C.; Righetto, S.; Roberto, D.; Ugo, R.; Valore, A.; Fantacci, S.; Sgamellotti, A.; De Angelis, F. *Chem. Commun.* **2007**, 4116 and references cited therein.

(13) (a) Goldsmith, J. I.; Hudson, W. R.; Lowry, M. S.; Anderson, T. H.; Bernhard, S. *J. Am. Chem. Soc.* **2005**, *127*, 7502. (b) Tinker, L. L.; McDaniel, N. D.; Curtin, P. N.; Smith, C. K.; Ireland, M. J.; Bernhard, S. *Chem.—Eur. J.* **2007**, *13*, 8726.

(14) For review, see: Lo, K. K.-W.; Hui, W.-K.; Chung, C.-K.; Tsang, K. H.-K.; Ng, D. C.-M.; Zhu, N.; Cheung, K.-K. *Coord. Chem. Rev.* **2005**, *249*, 1434 and references cited therein. For representative examples, see: (a) Lo, K. K.-W.; Chung, C.-K.; Zhu, N. *Chem.—Eur. J.* **2006**, *12*, 1500. (b) Lo, K. K.-W.; Zhang, K. Y.; Chung, C.-K.; Kwok, K. Y. *Chem.—Eur. J.* **2007**, *13*, 7110. (c) Shao, F.; Barton, J. K. *J. Am. Chem. Soc.* **2007**, *129*, 14733. (d) Elias, B.; Shao, F.; Barton, J. K. *J. Am. Chem. Soc.* **2008**, *130*, 1152. (e) Lau, J. S.-Y.; Lee, P.-K.; Tsang, K. H.-K.; Ng, C. H.-C.; Lam, Y.-W.; Cheng, S.-H.; Lo, K. K.-W. *Inorg. Chem.* **2009**, *48*, 708. (f) Dannany, L.; Forster, R. J.; White, B.; Smyth, M.; Rusling, J. F. *J. Am. Chem. Soc.* **2004**, *126*, 8835.

(15) Cheung, K.-M.; Zhang, Q.-F.; Chan, K.-W.; Lam, M. H. W.; Williams, I. D.; Leung, W.-H. *J. Organomet. Chem.* **2005**, *690*, 2913.

(16) For some representative examples, see: (a) Lo, K. K.-W.; Chung, C.-K.; Zhu, N. *Chem.—Eur. J.* **2003**, *9*, 475. (b) Geiss, B.; Lambert, C. *Chem. Commun.* **2009**, 1670. (c) Lo, K. K.-W.; Lau, J. S.-Y. *Inorg. Chem.* **2007**, *46*, 700.

(17) For some representative examples, see: (a) Gross, E. M.; Armstrong, N. R.; Wightman, R. M. *J. Electrochem. Soc.* **2002**, *149*, E13. (b) Muegge, B. D.; Richter, M. M. *Anal. Chem.* **2004**, *76*, 73. (c) Kapturkiewicz, A.; Nowacki, J.; Borowicz, P. *Z. Phys. Chem.* **2006**, *220*, 525. (d) Kim, J. I.; Shin, I.-S.; Kim, H.; Lee, J.-K. *J. Am. Chem. Soc.* **2005**, *127*, 1614. (e) Miao, W. *Chem. Rev.* **2008**, *108*, 2506. (f) Richter, M. M. *Chem. Rev.* **2004**, *104*, 3003. (g) Kapturkiewicz, A.; Angulo, G. *J. Chem. Soc., Dalton Trans.* **2003**, 3907.

(18) (a) Albano, V. G.; Bandini, M.; Barbarella, G.; Melucci, M.; Monari, M.; Piccinelli, F.; Tommasi, S.; Umani-Ronchi, A. *Chem.—Eur. J.* **2006**, *12*, 667. (b) Melucci, M.; Barbarella, G.; Gazzano, M.; Cavallini, M.; Biscarini, F.; Bongini, A.; Piccinelli, F.; Monari, M.; Bandini, M.; Umani-Ronchi, A.; Biscarini, P. *Chem.—Eur. J.* **2006**, *12*, 7304. (c) Albano, V. G.; Bandini, M.; Moorlag, C.; Piccinelli, F.; Pietrangelo, A.; Tommasi, S.; Umani-Ronchi, A.; Wolf, M. O. *Organometallics* **2007**, *26*, 4373. (d) Bandini, M.; Pietrangelo, A.; Sinisi, R.; Umani-Ronchi, A.; Wolf, M. O. *Eur. J. Org. Chem.* **2009**, 3554.

(19) Mishra, A.; Ma, C.-Q.; Bäuerle, P. *Chem. Rev.* **2009**, *109*, 1141.

(20) (a) Kulikova, M. V.; McClenaghan, N.; Balashev, K. P. *Russ. J. Org. Chem.* **2005**, *75*, 665. (b) For a recent example of different coordination modes of 2-phenylthiophene in cyclometalated iridium complexes, see:Ren, X.; Giesen, D. J.; Rajeswaran, M.; Madaras, M. *Organometallics* **2009**, *28*, 6079.

Chart 1. Neutral and Cyclometalating Ligands Used in the Present Investigation

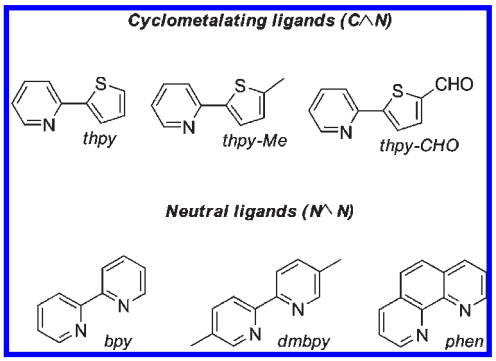

the solvent resonance as the internal standard (deuterochloroform: δ 7.27 ppm). Data are reported as follows: chemical shift, multiplicity (s = singlet, d = doublet, pd = pseudodoublet, t = triplet, q = quartet, br = broad, br s = broad singlet, m = multiplet), coupling constants (Hz). Gas chromatography−mass spectrometry (GC−MS) spectra were taken by electron impact ionization at 70 eV on a Hewlett-Packard 5971 with GC injection. They are reported as *m*/*z* (relative intensity). Liquid chromatography−electrospray ionization mass spectrometry (MS-ESI) spectra were obtained with an Agilent Technologies MSD1100 single-quadrupole mass spectrometer. Chromatographic purification was done with 240−400 mesh silica gel. IR analysis were performed with a FT-IR Nicolet 205 spectrophotometer, and the spectra are expressed by wavenumber (cm^{-1}). Elemental analyses were carried out by using a EACE 1110 CHNOS analyzer. Melting points were determined with a Büchi 150 melting point unit and are not corrected.

Materials. All anhydrous solvents were supplied by Fluka in Sureseal bottles and used as received. 2-Ethoxyethanol was distilled from $MgSO_4$. $IrCl_3 \cdot 3H_2O$ was supplied by Strem. 5-(2-Pyridyl)thiophene-2-carbaldehyde (thpy-CHO) was synthesized by following a known protocol.[21] 5-(2-Pyridyl)-2-methylthiophene (thpy-Me) was synthesized via a variant of ref 21: thpy (1 equiv), *n*-BuLi (1.1 equiv), MeI (1.1 equiv). Yield: 30% (not optimized). ^{1}H NMR ($CDCl_3$, 300 MHz): δ 2.55 (s, 3H), 6.79 (s, 1H), 7.10−7.13 (m, 1H), 7.28 (d, J = 3.3 Hz, 1H), 7.38−7.42 (m, 1H), 7.60−7.67 (m, 1H), 8.55 (s, 1H). GC−MS: *m*/*z* 51 (10), 78 (9), 97 (12), 130 (19), 141 (17), 175 (100, M). dmbpy = 5,5′-dimethyl-2,2′-dipyridyl, thpy = 2-thienylpyridine, phen = 1,10-phenanthroline, and 2,2′-bipyridine (bpy) were procured from commercial sources and used without further purification.

Synthesis of the Cationic Cyclometalated Iridium(III) Complexes.[22] To a degassed ethoxyethanol/water mixture (3:1, 4 mL) were added 100 mg (0.28 mmol) of $IrCl_3 \cdot 3H_2O$ and 0.70 mmol (2.5 equiv) of the desired carbometalable ligand (thpy, thpy-CHO, or thpy-Me). The mixture was refluxed overnight (~16 h) and then cooled down. The volatiles were removed under reduced pressure, and the deep-red solid was recovered by centrifugation. The resulting solid was washed with water (20 mL) and diethyl ether (20 mL) and recovered by centrifugation. The resulting deep-red solid was dissolved in CH_2Cl_2. Traces of insoluble material were removed by filtration. Evaporation of the solvent led to a red-orange solid, which was used without any further purification.

$[Ir(thpy)_2Cl]_2$ (**1a**).[23] Yield: 68% (115 mg). ^{1}H NMR ($CDCl_3$, 200 MHz): δ 5.92 (d, J = 5.2 Hz, 4H), 6.62 (dt, J_1 = 1.4 Hz, J_2 = 7.4 Hz, 4H), 7.06 (d, J = 5.2 Hz, 4H), 7.50 (d, J = 7.0 Hz, 4H), 7.60 (dd, J_1 = 1.4 Hz, J_2 = 7.4 Hz, 4H), 9.00 (d, J = 5.8 Hz, 4H).

$[Ir(thpy\text{-}CHO)_2Cl]_2$ (**1b**). Yield: 90% (137 mg). ^{1}H NMR (CD_2Cl_2, 300 MHz): δ 6.57 (s, 4H), 6.92 (t, J = 5.7 Hz, 4H), 7.80−7.92 (m, 8H), 9.15 (d, J = 6.0 Hz, 4H), 9.65 (s, 4H).

$[Ir(thpy\text{-}Me)_2Cl]_2$ (**1c**). Yield: 69% (120 mg). ^{1}H NMR ($CDCl_3$, 300 MHz): δ 2.28 (s, 12H), 5.64 (br s, 4H), 6.55 (t, J = 9.3 Hz, 4H), 7.37 (d, J = 12.0 Hz, 4H), 7.53−7.61 (m, 4H), 8.90 (d, J = 7.8 Hz, 4H).

To a solution of **1** (1 equiv) in 20 mL of a degassed CH_2Cl_2/MeOH (1:1) mixture was added all at once 2 equiv of a bis-imine ligand (N^N), and the mixture was stirred in the dark for 4 h at reflux. The red solution was then cooled to room temperature, anhydrous NH_4PF_6 was added (4 equiv), and the mixture was stirred overnight in the dark at room temperature. After evaporation of the solvent under reduced pressure, 25 mL of H_2O was added with the aim of removing excess NH_4PF_6. The solid obtained was washed with diethyl ether (20 mL) and dried under vacuum.

$[Ir(thpy)_2bpy]PF_6$, starting from 0.067 mmol of **1a**. Yield: 77% (82 mg). MS-ESI: *m*/*z* 669 ($[Ir(thpy)_2bpy]^+$). ^{1}H NMR (CD_2Cl_2, 200 MHz): δ 6.37 (d, J = 4.4 Hz, 2H), 6.83 (t, J = 6.4 Hz, 2H), 7.40 (d, J = 5.8 Hz, 2H), 7.46 (d, J = 4.8 Hz, 2H), 7.53 (d, J = 5.4 Hz, 2H), 7.59 (d, J = 6.2 Hz, 2H), 7.72−7.77 (m, 2H), 7.98 (d, J = 4.4 Hz, 2H), 8.14 (t, J = 7.6 Hz, 2H), 8.49 (d, J = 8.4 Hz, 2H). Elem anal. Calcd for $C_{28}H_{20}F_6IrN_4PS_2$: C, 41.32; H, 2.48; N, 6.88. Found: C, 41.40; H, 2.44; N, 6.95.

$[Ir(thpy\text{-}CHO)_2bpy]PF_6$, starting from 0.074 mmol of **1b**. Yield: 81% (104 mg). MS-ESI: *m*/*z* 725 ($[Ir(thpy\text{-}CHO)_2bpy]^+$). ^{1}H NMR ($CDCl_3$, 300 MHz): δ 6.87 (s, 2H), 7.04 (dt, J_1 = 2.1 Hz, J_2 = 6.6 Hz, 2H), 7.50−7.58 (m, 4H), 7.77−7.83 (m, 4H), 8.04 (d, J = 5.4 Hz, 2H), 8.21 (t, J = 8.1 Hz, 2H), 8.55 (d, J = 8.4 Hz, 2H), 9.84 (s, 2H). Elem anal. Calcd for $C_{30}H_{20}F_6IrN_4O_2PS_2$: C, 41.42; H, 2.32; N, 6.44. Found: C, 41.51; H, 2.22; N, 6.55.

$[Ir(thpy\text{-}Me)_2bpy]PF_6$, starting from 0.064 mmol of **1c**. Yield: 50%. MS-ESI: *m*/*z* 637 ($[Ir(thpy\text{-}Me)_2bpy]^+$). ^{1}H NMR ($CDCl_3$, 300 MHz): δ 2.49 (s, 6H), 5.96 (s, 2H), 6.73−6.77 (m, 2H), 7.30 (d, J = 4.2 Hz, 2H), 7.39 (d, J = 8.1 Hz, 2H) 7.49−7.51 (m, 2H), 7.54−7.61 (m, 2H), 7.95−7.97 (m, 2H), 8.15 (t, J = 8.1 Hz, 2H), 8.64 (d, J = 8.1 Hz, 2H). Elem anal. Calcd for $C_{30}H_{24}F_6IrN_4PS_2$: C, 40.82; H, 2.87; N, 6.66. Found: C, 40.75; H, 2.78; N, 6.70.

$[Ir(thpy\text{-}CHO)_2dmbpy]PF_6$, starting from 0.020 mmol of **1b**. Yield: 67% (24 mg). MS-ESI: *m*/*z*753 ($[Ir(thpy\text{-}CHO)_2dmbpy]^+$). ^{1}H NMR ($CDCl_3$, 300 MHz): δ 2.32 (s, 6H), 6.85 (s, 2H), 7.17 (br s, 2H), 7.57 (br s, 2H), 7.65 (s, 2H), 7.79−7.84 (m, 4H), 7.95−7.99 (m, 2H), 8.50−8.53 (m, 2H), 9.83 (s, 2H). Elem anal. Calcd for $C_{32}H_{24}F_6IrN_4O_2PS_2$: C, 41.81; H, 2.69; N, 6.24. Found: C, 41.91; H, 2.56; N, 6.33.

$[Ir(thpy\text{-}CHO)_2phen]PF_6$, starting from 0.076 mmol of **1b**. Yield: 67%. MS-ESI: *m*/*z* 748 ($[Ir(thpy\text{-}CHO)_2phen]^+$), 145 ($[PF_6]^-$). ^{1}H NMR ($CD_3CN$, 200 MHz): δ 6.87 (dt, J_1 = 1.4 Hz, J_2 = 7.6 Hz, 2H), 7.10 (s, 2H), 7.42 (d, J = 5.8 Hz, 2H), 7.65−7.92 (m, 6H), 8.25 (s, 2H), 8.35 (dd, J_1 = 1.2 Hz, J_2 = 5.0 Hz, 2H), 8.70 (dd, J_1 = 1.2 Hz, J_2 = 8.6 Hz, 2H), 9.85 (s, 2H). Elem anal. Calcd for $C_{32}H_{20}F_6IrN_4O_2PS_2$: C, 43.00; H, 2.26; N, 6.27. Found: C, 42.90; H, 2.31; N, 6.35.

Crystal Data. The diffraction experiments were carried out at room temperature on a Bruker SMART Apex II CCD-based diffractometer using graphite-monochromated Mo Kα radiation (λ = 0.710 73 Å). Intensity data were measured over the full diffraction sphere using 0.3° wide ω scans. The software *SMART*[24] was used for collecting frames of data, indexing reflections, and determining the lattice parameters. The collected

(21) Nerenz, H.; Meier, M.; Grahn, W.; Reisner, A.; Schmaelzlin, E.; Stadler, S.; Meerholz, K.; Bräuchle, C.; Jones, P. G. *J. Chem. Soc., Perkin Trans. 2* **1998**, 437–448.

(22) Nonoyama, M. *Bull. Chem. Soc. Jpn.* **1974**, *47*, 767.

(23) (a) Colombo, M. G.; Güdel, H. U. *Inorg. Chem.* **1993**, *32*, 3081. (b) McGee, K. A.; Mann, K. R. *Inorg. Chem.* **2007**, *46*, 7800.

(24) *SMART & SAINT Software Reference Manuals* (*Windows NT Version*), version 5.051; Bruker Analytical X-ray Instruments Inc.: Madison, WI, 1998.

frames were then processed for integration by software *SAINT*,[24] and an empirical absorption correction was applied with *SADABS*.[25] The structures were solved by direct methods (SIR97)[26] and subsequent Fourier syntheses and refined by full-matrix least-squares calculations on F^2 (*SHELXTL*),[27] attributing anisotropic thermal parameters to all non-hydrogen atoms. The aldehydic and aromatic hydrogen atoms that were located on the Fourier difference map were placed in calculated positions and refined with idealized geometry with $U_{iso}(H) = 1.2U_{eq}(C)$. The complex $[Ir(thpy)_2bpy]PF_6$ crystallized with one-third of an ordered water molecule and a lattice solvent (presumably MeOH) could not be modeled reasonably, so the *SQUEEZE* routine found in *PLATON* was used. $[Ir(thpy\text{-}CHO)_2bpy]PF_6$ and $[Ir(thpy\text{-}CHO)_2phen]PF_6$ crystallized with solvent molecules (dichloromethane, DCM). Crystal data and experimental details are reported in Table S1 (Supporting Information).

CCDC-737663−CCDC-737665 contain the supplementary crystallographic data for this paper. These data can be obtained free of charge from the Cambridge Crystallographic Data Centre via www.ccdc.cam.ac.uk/data_request/cif.

Electrochemical Measurements. Tetrabutylammonium hexafluorophosphate (TBAH; electrochemical grade from Fluka) was used as received as a supporting electrolyte. Acetonitrile (ACN), DCM, and tetrahydrofuran (THF) were purified and dried as previously reported,[28] stored in a specially designed Schlenk flask, and protected from light.

All of the solvents were distilled via a closed system into an electrochemical cell, containing the supporting electrolyte and the species under examination, immediately before the experiment was performed. Electrochemical experiments were carried out in an airtight single-compartment cell described elsewhere,[28] using platinum as the working and counter electrodes and a silver spiral as a quasi-reference electrode. The drift of the quasi-reference electrode was negligible during the time required for an experiment. All of the $E_{1/2}$ potentials have been directly obtained from cyclic voltammetric (CV) curves as averages of the cathodic and anodic peak potentials and by digital simulation for those processes, which are not Nernstian, or for processes closely spaced in multielectron voltammetric peaks. The $E_{1/2}$ values, referenced to the saturated calomel electrode (SCE), have been determined by adding ferrocene at the end of each experiment as an internal standard and measuring them with respect to the ferrocinium/ferrocene couple standard potential. The temperature-dependent ferrocinium/ferrocene couple standard potential was measured with respect to SCE by a nonisothermal arrangement according to the method outlined by Weaver et al.[29] The potentials thus obtained were not corrected for the unknown liquid junction potential between the organic phase and the aqueous SCE solution.

The cell containing the supporting electrolyte and the electroactive compound was dried under a vacuum at 100−120 °C for at least 60 h before each experiment. The pressure measured in the electrochemical cell prior to trap-to-trap distillation of the solvent was typically $(1-2) \times 10^{-5}$ mbar. Voltammograms were recorded with an AMEL model 552 potentiostat or a custom-made fast potentiostat[30] controlled by an AMEL model 568 programmable function generator. The potentiostat was interfaced to a Nicolet model 3091 digital oscilloscope, and the data were transferred to a personal computer by the program *Antigona*.[31] Minimization of the uncompensated resistance effect in the voltammetric measurements was achieved by the positive-feedback circuit of the potentiostat. Digital simulations of the CV curves were carried out by either Antigona or DigiSim 3.0. Determination of the potentials, for the irreversible processes, was obtained by digital simulation of the CV curves,[32] utilizing a best-fitting procedure of the experimental curves recorded at different scan rates spanning over, at least, 2 orders of magnitude.

Absorption and Emission Spectroscopy and ECL. UV−visible absorption spectra were recorded on a UV−vis−near-IR spectrophotometer (Varian CARY5). Photoluminescence (PL) measurements were performed with a Varian (Cary Eclipse) spectrofluorimeter. The absorbance and luminescence spectra of the complexes were obtained in ACN solutions. The relative luminescence efficiency was measured using an optically diluted ACN solution (OD < 0.1 at the excitation wavelength) and calibrated with $Ru(bpy)_3^{2+}$ as a standard according to the procedure reported elsewhere.[33]

The ECL measurements were carried out in an ACN solution with TBAH as the supporting electrolyte, under the same strictly aprotic conditions as those described above, in the Electrochemical Measurements section. A one-compartment three-electrode airtight cell, with high-vacuum O-rings and glass stopcocks, was used for ECL measurements.[34] The working electrode consisted of a platinum side-oriented, 2-mm-diameter disk sealed in glass while the counter electrode was a platinum spiral and the reference electrode was a quasi-reference silver wire.

For a given solution, two or three records were made to check the temporal stability of the system investigated.

The annihilation reaction was obtained by pulsing the working electrode between the first oxidation and first reduction peak potentials of the complex with a pulse width of 0.1 s. The ECL signal generated by the potential step program was measured with a photomultiplier tube (PMT; Hamamatsu R4220p) placed a few millimeters from the cell, and in front of the working electrode, inside a darkbox. A voltage in the range of 750−1000 V was supplied to the PMT. The light/current/voltage curves were recorded by collection of the preamplified PMT output signal (using an ultralow-noise Acton Research model 181), with the second input channel of the ADC module of the Autolab instrument, without any correction for the PMT response at different wavelengths. ECL spectra have been recorded by insertion of the same PMT in a dual-exit monocromator (Acton Research model Spectra Pro2300i) and collection of the signal as described above. The photocurrent detected at the PMT was accumulated for 1−3 s, depending on the emission intensity, for each monocromator wavelength step (usually 1 nm). Entrance and exit slits were fixed to the maximum value of 3 mm.

(25) Sheldrick, G. M. *SADABS, program for empirical absorption correction*; University of Göttingen: Göttingen, Germany, 1996.
(26) Altomare, A.; Burla, M. C.; Cavalli, M.; Cascarano, G. L.; Giacovazzo, C.; Guagliardi, A.; Moliterni, A. G. G.; Polidori, G.; Spagna, R. *J. Appl. Crystallogr.* **1999**, *32*, 115.
(27) Sheldrick, G. M. *SHELXTLplus* (*Windows NT version*) *Structure Determination Package*, version 5.1; Bruker Analytical X-ray Instruments Inc.: Madison, WI, 1998.
(28) (a) Bruno, C.; Benassi, R.; Passalacqua, A.; Paolucci, F.; Fontanesi, C.; Marcaccio, M.; Jackson, E. A.; Scott, L. T. *J. Phys. Chem. B* **2009**, *113*, 1954. (b) La Pensée, A. A.; Bickley, J.; Higgins, S. J.; Marcaccio, M.; Paolucci, F.; Roffia, S.; Charnock, J. M. *J. Chem. Soc., Dalton Trans.* **2002**, 4095. (c) Guldi, D. M.; Maggini, M.; Menna, E.; Scorrano, G.; Ceroni, P.; Marcaccio, M.; Paolucci, F.; Roffia, S. *Chem.—Eur. J.* **2001**, *7*, 1597.
(29) Yee, E. L.; Cave, R. J.; Guyer, K. L.; Tyma, P. D.; Weaver, M. J. *J. Am. Chem. Soc.* **1979**, *101*, 1131.
(30) Amatore, C.; Lefrou, C. *J. Electroanal. Chem.* **1992**, *324*, 33.
(31) Mottier, L. *Antigona*; University of Bologna: Bologna, Italy, **1999**.
(32) Spieser, B. In *Electroanalytical Chemistry. A Series of Advances*; Bard, A. J., Rubistein, I., Eds.; Marcel Dekker, Inc.: New York, 1996; Vol. *19*, p 1 and references cited therein.
(33) Stagni, S.; Colella, S.; Palazzi, A.; Valenti, G.; Zacchini, S.; Paolucci, F.; Marcaccio, M.; Albuquerque, R. Q.; De Cola, L. *Inorg. Chem.* **2008**, *47*, 10509.
(34) (a) Zanarini, S.; Della Ciana, L.; Marcaccio, M.; Marzocchi, E.; Paolucci, F.; Prodi, L. *J. Phys. Chem. B* **2008**, *112*, 10188. (b) Stagni, S.; Palazzi, A.; Zacchini, S.; Ballarin, B.; Bruno, C.; Marcaccio, M.; Paolucci, F.; Monari, M.; Carano, M.; Bard, A. J. *Inorg. Chem.* **2006**, *45*, 695.

ECL yields were determined against the annihilation reaction of a standard ECL system [i.e., $Ru(bpy)_3^{2+}$] in an ACN solution containing TBAH. The ECL yields were obtained by a chronoamperometric experiment using the following expression:[35]

$$\Phi_{ECL} = \Phi_{ECL}^{\circ}(IQ^{\circ}/I^{\circ}Q)$$

where Φ_{ECL}° is the ECL efficiency of the standard under the same experimental conditions ($\Phi_{ECL}^{\circ} = 0.05$),[36] I and I° are the integrated ECL intensities of the compound and standard systems, and Q and Q° are the charges (in Coulombs) passed for the complex and standard species, respectively. It has been estimated that the ECL efficiency can be confidently given with an error of 15%.

Results and Discussion

The development of new functionalized bis-cyclometalated iridium(III) complexes is currently of considerable interest. Many advances in this endeavor have focused on the introduction of binding sites on the ancillary neutral ligands.[6a,37] However, the search for unprecedented tailor-designed functionalization of cyclometalating ligands that allow increasingly rapid access to structural complexity remains a preeminent goal.[16] Finally, although the emission color of such a class of iridium complexes is generally governed by the cyclometalating ligand, also neutral bis-pyridine (ancillary) ligands have been demonstrated to actually affect both the quantum yield and emission color tunability of iTMCs.[38] Therefore, for a systematic investigation, several bis-imine type ligands (e.g. bpy, dmbpy, and phen) were taken into account. Electron-withdrawing formyl groups are known to strongly affect all of the electronic properties of cationic mixed-ligand iridium complexes $[(C^{\wedge}N)_2Ir(N^{\wedge}N)]^+$, and to adequately assess such a role, unsubstituted (thpy) and complementary (thpy-Me) ligands were also considered.

The target iridium μ-chloro-bridged dimers of the general formula $(C^{\wedge}N)_2Ir(\mu\text{-}Cl)_2Ir(C^{\wedge}N)_2$ were obtained in good-to-excellent yields (68−90%) via a known protocol that involves the treatment of $IrCl_3 \cdot 3H_2O$ with an excess of the desired cyclometalating ligand (thpy, thpy-CHO, and thpy-Me) in a solvent mixture of ethoxyethanol/water (Scheme 1).[22]

Finally, the cationic bis-cyclometalated complexes were obtained by reaction of the dimers (**1**) with the bis-imine ligands ($N^{\wedge}N$) in a CH_2Cl_2/MeOH mixture, followed by a metathesis reaction with NH_4PF_6 (Scheme 2). The deep-red air-stable complexes were isolated in moderate-to-good yields (50−81%) and were fully characterized by HPLC-MS and ^1H NMR analysis. High-purity samples of complexes for electrochemical, spectroscopic, and luminescence investigations were obtained by crystallization.

Crystals suitable for X-ray diffraction experiments have been obtained for $[Ir(thpy)_2bpy]PF_6$, $[Ir(thpy\text{-}CHO)_2bpy]PF_6$, and $[Ir(thpy\text{-}CHO)_2phen]PF_6$ by the slow diffusion of hexane into CH_2Cl_2 solutions of the complexes at room

Scheme 1. Synthesis of the μ-Chloro-Bridged Dimers **1a**−**1c**

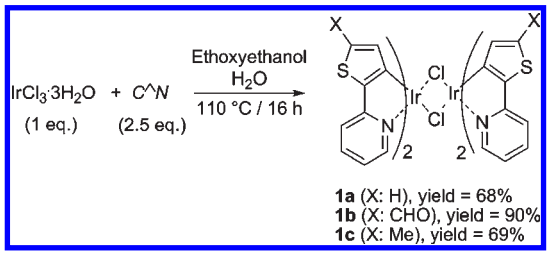

Scheme 2. Synthesis of the Cationic Cyclometalated Iridium(III) Complexes

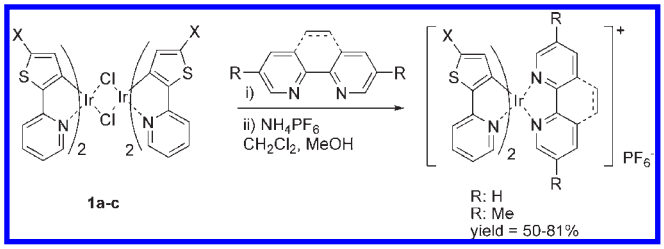

temperature. In all three structures, iridium(III) adopts a distorted octahedral geometry, with the C and N atoms belonging to cyclometalated ligands in *cis* and *trans* configurations, respectively (Figure 2).

The nitrogen atoms of the bis-imine ligands are in *trans* to the carbon ones, and the Ir−N(bis-imine) bond lengths fall in the range of 2.114−2.141 Å (Table 1). These distances are significantly longer than the Ir−N(thpy) bond lengths (range 2.031−2.072 Å) in mutual *trans* positions, in agreement with what is usually observed for related compounds.[39] This behavior is ascribable to the stronger *trans* influence of the sp^2 σ-donor carbon with respect to the sp^2 nitrogen of unsaturated α,α'-bis-imine (bpy and phen).

The Ir−C bond distances (1.995−2.018 Å) are within the interval observed for the corresponding distance in iridium-(III) $C^{\wedge}N$ chelates with similar geometry and ligand environments.[40] The bite angles of the thpy ligands (79.7−80.2°) in $[Ir(thpy)_2bpy]PF_6$, $[Ir(thpy\text{-}CHO)_2bpy]PF_6$, and $[Ir(thpy\text{-}CHO)_2phen]PF_6$ lie in the same range as that observed in the literature for similar complexes. The bite angles of the bis-imine ligands (range 76.9−78.3°) are in the same range as that reported earlier for Ir^{III}bpy fragments.[41]

It is worth mentioning that incorporation of the aldehyde function in the 5′ position of the thpy ligand does not change significantly the bond lengths involving the metal center. On the contrary, coordination of the phen ring, with respect to the bpy one, leads to a slight shortening of the Ir−N(thpy) bond [2.031(16) Å]. In addition, in the crystal structures of $[Ir(thpy\text{-}CHO)_2bpy]PF_6$ and $[Ir(thpy\text{-}CHO)_2phen]PF_6$, the CHO functions are coplanar with the thpy-conjugated system with a *cis* arrangement of O1 with respect to S1.

(35) *Electrogenerated Chemiluminescence*; Bard, A. J., Ed.; Marcel Dekker: New York, 2004.
(36) Rubinstein, L.; Bard, A. J. *J. Am. Chem. Soc.* **1981**, *103*, 6641.
(37) (a) Neve, F.; Crispini, A.; Campagna, S.; Serroni, S. *Inorg. Chem.* **1999**, *38*, 2250. (b) Neve, F.; Crispini, A. *Eur. J. Inorg. Chem.* **2000**, 1039. (c) Plummer, E. A.; Hofstraat, J. W.; De Cola, L. *J. Chem. Soc., Dalton Trans.* **2003**, 2080. (d) Neve, F.; La Deda, M.; Crispini, A.; Bellusci, A.; Puntoriero, F.; Campagna, S. *Organometallics* **2004**, *23*, 5856.
(38) Dragonetti, C.; Falciola, L.; Mussini, P.; Righetto, S.; Roberto, D.; Ugo, R.; Valore, A.; De Angelis, F.; Fantacci, S.; Sgamellotti, A.; Ramon, M.; Muccini, M. *Inorg. Chem.* **2007**, *46*, 8533.
(39) (a) van Diemen, J. H.; Haasnoot, J. G.; Hage, R.; Müller, E.; Reedijk, J. *Inorg. Chim. Acta* **1991**, *181*, 245. (b) Garces, F. O.; Dedeian, K.; Keder, N. L.; Watts, R. J. *Acta Crystallogr.* **1993**, *C49*, 1117. (c) Nord, G.; Hazell, A. C.; Hazell, R. G.; Farver, O. *Inorg. Chem.* **1983**, *22*, 3429. (d) Urban, R.; Kramer, R.; Shahram, M.; Polborn, K.; Wagner, B.; Beck, W. *J. Organomet. Chem.* **1996**, *517*, 191.
(40) Colombo, M.-G.; Brunold, T.-C.; Riedner, T.; Güdel, H. U.; Förtsch, M.; Bürgi, H.-B. *Inorg. Chem.* **1994**, *33*, 545.
(41) (a) Hazell, A. C.; Hazell, R. G. *Acta Crystallogr.* **1984**, *C40*, 806. (b) Alexander, B. D.; Johnson, B. J.; Johnson, S. M.; Boyle, P. D.; Kann, N. C.; Mueting, A. M.; Pignolet, L. H. *Inorg. Chem.* **1987**, *26*, 3506. (c) Albano, V. G.; Bellon, P. L.; Sansoni, M. *Inorg. Chem.* **1969**, *8*, 298.

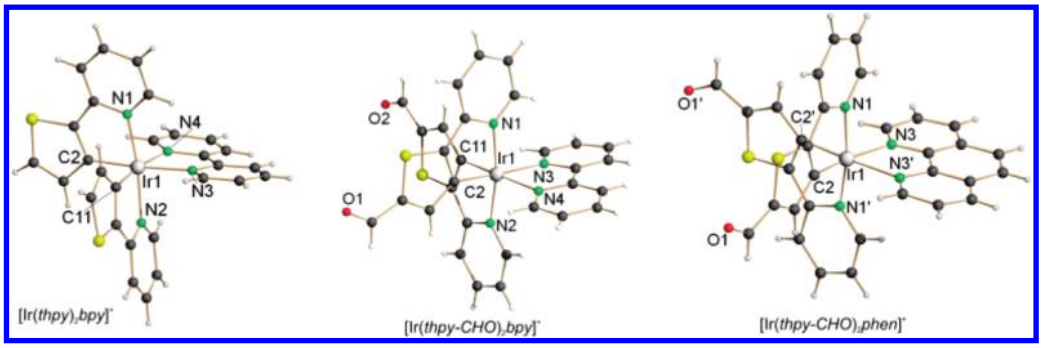

Figure 2. Crystal structures of the cations of $[Ir(thpy)_2bpy]PF_6$, $[Ir(thpy\text{-}CHO)_2bpy]PF_6$, and $[Ir(thpy\text{-}CHO)_2phen]PF_6$. The PF_6 anion and the crystallization solvents are omitted for clarity. The primed atoms in $[Ir(thpy\text{-}CHO)_2phen]PF_6$ are generated by a symmetry operation (symmetry code: I, $-x + {}^1/_2, y, -z + {}^3/_2$).

Table 1. Selected Bond Lengths (Å) and Angles (deg) for $[Ir(thpy)_2bpy]PF_6$, $[Ir(thpy\text{-}CHO)_2bpy]PF_6$, and $[Ir(thpy\text{-}CHO)_2phen]PF_6$[a]

	$[Ir(thpy)_2bpy]PF_6$	$[Ir(thpy\text{-}CHO)_2bpy]PF_6$		$[Ir(thpy\text{-}CHO)_2phen]PF_6$
Ir1−N1	2.072(4)	2.066(2)	Ir1−N1	2.031(16)
Ir1−C2	1.998(5)	1.995(3)	Ir1−C2	2.018(19)
Ir1−N2	2.063(4)	2.064(2)	Ir1−N3	2.141(14)
Ir1−C11	2.006(5)	2.002(3)		
Ir1−N3	2.124(4)	2.128(3)		
Ir1−N4	2.114(4)	2.116(2)		
N1−Ir1−C2	80.2(2)	80.00(11)	N1−Ir1−C2[a]	79.7(6)
N2−Ir1−C11	79.9(2)	80.19(11)	N3−Ir1−N3[a]	78.3(9)
N3−Ir1−N4	77.2(2)	76.85(9)	N1−Ir1−N1[a]	172.9(8)
N1−Ir1−N2	170.6(2)	169.69(9)	N3−Ir1−C2[a]	173.0(6)
N3−Ir1−C2	171.4(2)	173.44(10)		
N4−Ir1−C11	173.0(2)	173.99(11)		

[a] Symmetry transformations used to generate equivalent atoms: $-x + {}^1/_2, y, z + {}^3/_2$.

Electronic Absorption Spectroscopy and Luminescence Properties. The absorption spectra of all complexes were recorded at room temperature in an ACN solution and are reported in Figure 3. The UV region displays the ligand-centered (LC) $^1\pi \rightarrow \pi^*$ transitions as the most intense absorption bands, for each species (Table 2). The shoulders appearing in the range of 350−450 nm are likely due to charge-transfer (CT) transitions, with their nature being both spin-allowed (singlet-to-singlet metal-to-ligand charge transfer, ^{1}MLCT) and spin-forbidden (singlet-to-triplet metal-to-ligand charge transfer, ^{3}MLCT). The relatively high intensity of these latter bands can be rationalized by the strong spin−orbit coupling effect, arising from the presence of a third-row transition metal in a high oxidation state such as iridium(III).[42]

All of the complexes are luminescent at room temperature in an ACN solution, with emission maxima of around 600 nm. In particular, among the series represented by the three aldehyde-containing compounds, e.g., $[Ir(thpy\text{-}CHO)_2bpy]^+$, $[Ir(thpy\text{-}CHO)_2dmbpy]^+$, and $[Ir(thpy\text{-}CHO)_2phen]^+$, the PL spectra display vibronic-structured emission bands, whereas for the remaining two species, the vibronic structure, although still present, is less evident. According to the published works concerning analogous iridium(III) cyclometalates,[43,44] the occurrence of a similar emission shape is attributed to the presence of an excited state resulting from the mixing of comparable percentages of ^{3}LC and ^{3}MLCT states. Similar results were very recently obtained for a series of iridium(III) tetrazolate species,[33] for which enhancement of the ^{3}LC−^{3}MLCT energy gap, due to replacement of a more electron-withdrawing ligand, makes the emission a structureless band, consistent with the prevalent ^{3}MLCT character of the excited state.

In a degassed ACN solution, the complexes reported here show emission quantum yields (Φ) ranging from 1.8%, as in the case of $[Ir(thpy\text{-}CHO)_2bpy]^+$, to 0.5% for the thpy complexes. The appreciable decrease of the quantum yield values, which is observed in air-equilibrated solutions, provides confirmation of the triplet character of the emissions. The introduction of the formyl group onto the thpy ligands stabilizes the occupied and virtual molecular orbitals with a consequent red shift of the emission band. Interestingly, the quantum yield of PL is much lower because the emission occurs at lower wavelength (i.e., $[Ir(thpy)_2bpy]^+$ and $[Ir(thpy\text{-}Me)_2bpy]^+$), according to the energy gap law.[43]

Electrochemical Behavior. The electrochemical properties of the cyclometalated complexes were investigated in ACN, DCM, and THF solutions by cyclic voltammetry, at room temperature. As previously reported[33,38,45] and

(42) Colombo, M. G.; Hauser, A.; Güdel, H. U. *Top. Curr. Chem.* **1994**, *171*, 143.
(43) (a) Flamigni, L.; Barbieri, A.; Sabatini, C.; Ventura, B.; Barigelletti, F. *Top. Curr. Chem.* **2007**, *281*, 143 and references cited therein. See also: (b) Dixon, I. M.; Collin, J.-P.; Sauvage, J.-P.; Flamigni, L.; Encinas, S.; Barigelletti, F. *Chem. Soc. Rev.* **2000**, *29*, 385.
(44) (a) Tsuboyama, A.; Iwawaki, H.; Furugori, M.; Mukaide, T.; Kamatani, J.; Igawa, S.; Moriyama, T.; Miura, S.; Takiguchi, T.; Okada, S.; Hoshino, M.; Ueno, K. *J. Am. Chem. Soc.* **2003**, *125*, 12971. (b) Orselli, E.; Kottas, G. S.; Konradsson, A. E.; Coppo, P.; Fröhlich, R.; De Cola, L.; van Dijken, A.; Büchel, M.; Börner, H. *Inorg. Chem.* **2007**, *46*, 11082.
(45) (a) Nazeeruddin, Md. K.; Wegh, R. T.; Zhou, Z.; Klein, C.; Wang, Q.; De Angelis, F.; Fantacci, S.; Grätzel, M. *Inorg. Chem.* **2006**, *45*, 9245.

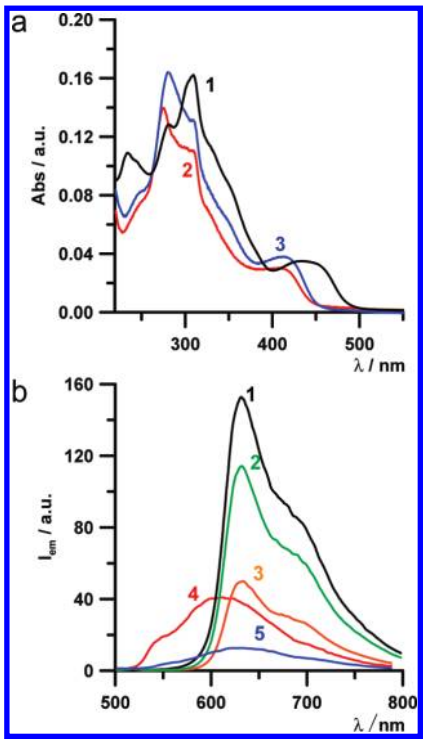

Figure 3. Absorption and emission spectra of the complexes in an ACN solution (0.2 mM) at 25 °C. (a) Absorption spectra: **1** (black line), $[Ir(thpy\text{-}CHO)_2bpy]^+$; **2** (red line), $[Ir(thpy)_2bpy]^+$; **3** (blue line), $[Ir(thpy\text{-}Me)_2bpy]^+$. (b) Emission spectra: **1** (black line), $[Ir(thpy\text{-}CHO)_2bpy]^+$; **2** (green line), $[Ir(thpy\text{-}CHO)_2phen]^+$; **3** (orange line), $[Ir(thpy\text{-}CHO)_2dmbpy]^+$; **4** (red line), $[Ir(thpy)_2bpy]^+$; **5** (blue line), $[Ir(thpy\text{-}Me)_2bpy]^+$.

Table 2. Adsorption and Emission Data for the Iridium Complexes Investigated in an ACN Solution at 25 °C

species	absorption λ_{abs} (nm)	emission λ_{em} (nm)	Φ_{Ph} (%)[a]
$[Ir(thpy\text{-}CHO)_2bpy]PF_6$	282, 309, 433	633	1.8
$[Ir(thpy)_2bpy]PF_6$	275, 309, 408	612	0.9
$[Ir(thpy\text{-}CHO)_2dmbpy]PF_6$	276, 312, 438	636	1.1
$[Ir(thpy\text{-}CHO)_2phen]PF_6$	273, 309, 436	633	1.8
$[Ir(thpy\text{-}Me)_2bpy]PF_6$	280, 308, 410	623	0.5

[a] QE of degassed solutions.

also shown by the density functional theory (DFT) calculations (vide infra), the electronic structures of these iridium species are characterized by a delocalization of the frontier molecular orbitals over both the metal and ligands. Accordingly, the oxidation of this class of iridium(III) species can be mainly attributed to the metal center, with a substantial contribution from the ligands, while, conversely, the reduction processes are mainly localized on the ligands, with only a partial contribution from the metal center. The potentials of the various processes are collected in Table 3. In the region of positive potential, explored up to about 1.5 V, all of the complexes exhibited a single one-electron reversible oxidation process. Conversely, in the negative potential region, all of the complexes display a rich voltammetric pattern largely associated with the reduction of both the cyclometalating ligand and the ancillary ligands. As an example, the CV curve of the complex $[Ir(thpy)_2bpy]^+$ is shown in Figure 4a, where four subsequent reduction peaks are

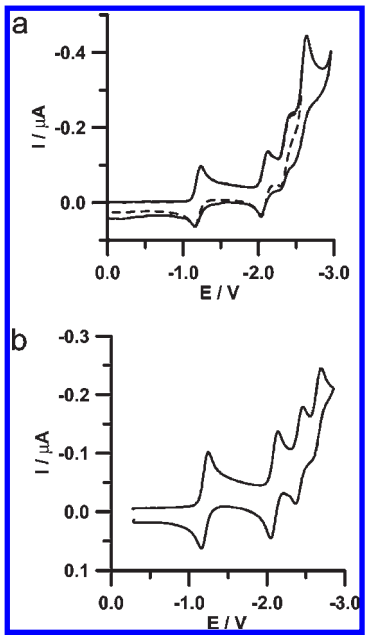

Figure 4. CV curves of a 1 mM solution of complexes (a) $[Ir(thpy)_2bpy]^+$ and (b) $[Ir(thpy\text{-}Me)_2bpy]^+$ in a 0.07 M TBAH/THF electrolyte (working electrode, platinum disk, 125 μm diameter; T = 25 °C; scan rate = 1 V/s).

observed. While the first three peaks correspond to reversible one-electron reductions, the fourth is irreversible likely because of a follow-up reaction coupled to the reduction process. The introduction of the methyl group on the cyclometalating ligand (e.g., 2-(5-methylthiophen-2yl)pyridine) ≡ thpy-Me; see the species $[Ir(thpy\text{-}Me)_2bpy]^+$) changed the CV pattern of the corresponding iridium species only slightly (Figure 4b). In particular, while the first reduction peak remained virtually unaffected by the substitution, a negative shift (by 20 and 60 mV, respectively) of the second and third reductions was observed (Table 3). This would suggest that the first reduction is localized into the ancillary ligand (bpy) and the second and third ones into the cyclometalating ligand. The fourth cathodic peak would then correspond to the second reduction of the bpy ligand, a process that is known to often trigger follow-up reactions that would explain the irreversible character of this peak.[46]

The above attribution of reduction processes was confirmed by replacement of the (weak) electron-donating methyl group by a strong electron acceptor, namely, aldehyde. Figure 5a shows the CV curve of complex $[Ir(thpy\text{-}CHO)_2bpy]^+$. The first reduction is still occurring at about the same potential, although slightly less negative (−1.1 V), as a consequence of the *second-order effect* of the −CHO substituents on the thpy ligands. Then, two one-electron closely spaced processes follow at about −1.5 V, and further three CV peaks can be observed in the last part of the CV curve, before solvent/electrolyte breakthrough. The two overlapping reduction peaks (i.e., the second and third processes at about −1.5 V) can be confidently attributed as the first process onto the

(46) (a) Krejčik, M.; Vlček, A. A. *J. Electroanal. Chem.* **1991**, *313*, 243. (b) Roffia, S.; Marcaccio, M.; Paradisi, C.; Paolucci, F.; Balzani, V.; Denti, G.; Serroni, S.; Campagna, S. *Inorg. Chem.* **1993**, *32*, 3003. (c) Marcaccio, M.; Paolucci, F.; Fontanesi, C.; Fioravanti, G.; Zanarini, S. *Inorg. Chim. Acta* **2007**, *360*, 1154.

Table 3. Half-Wave ($E_{1/2}$) Redox Potentials (vs SCE) of Uncoordinated Ligands and Iridium Complexes at 25 °C

species	$E_{1/2}$(ox) (V)[a]	$E_{1/2}$(red) (V)[b] I	II	III	IV	V	VI
thpy		−2.27	−2.86[c]				
thpy-CHO		−1.48	−2.01				
$[Ir(thpy\text{-}CHO)_2bpy]^+$	1.42	−1.14	−1.40	−1.49	−1.99	−2.21	−2.57
$[Ir(thpy)_2bpy]^+$	1.20	−1.19	−2.08	−2.35	−2.53[c]		
$[Ir(thpy\text{-}CHO)_2dmbpy]^+$	1.40	−1.25	−1.40	−1.60	−2.05	−2.30	−2.68
$[Ir(thpy\text{-}CHO)_2phen]^+$	1.41	−1.17	−1.41	−1.53	−2.02	−2.26	−2.51
$[Ir(thpy\text{-}Me)_2bpy]^+$	1.07	−1.19	−2.10	−2.41	−2.64[c]		

[a] Oxidation potentials measured in a DCM solution. [b] Reduction processes measured in a THF solution. [c] Irreversible process whose $E_{1/2}$ potential has been determined by digital simulation of the CV curve.

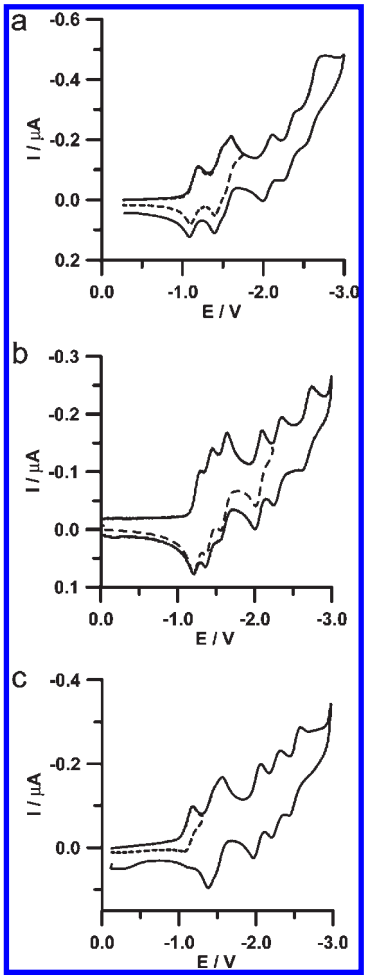

Figure 5. CV curves of a 1 mM solution of complexes (a) $[Ir(thpy\text{-}CHO)_2bpy]^+$, (b) $[Ir(thpy\text{-}CHO)_2dmbpy]^+$, and (c) $[Ir(thpy\text{-}CHO)_2phen]^+$, in a 0.08 M TBAH/THF electrolyte (working electrode, platinum disk, 125 μm diameter; T = 25 °C; scan rate = 1 V/s).

two thpy-CHO ligands, as is further explained below and also on the basis of the quantum mechanical calculations (vide infra). The redox behavior of the uncoordinated ligands allowed one to attribute the successive two reductions of the CV curve as the electron pairing onto the thpy ligands while the last process is the second reduction of the bpy ligand. The last process is affected by a follow-up reaction, and it becomes more reversible as the scan rate is increased.

In Figure 5b,c, the CV curves of the two homologous iridium species, where only the ancillary ligand bpy has been changed, are shown. When bpy is replaced with dmbpy, the first reduction moves toward more negative potentials and the following two closely spaced processes are split into two well-defined CV peaks. Again, a different electronic modulation of the ancillary ligand by replacement of bpy with another one, in this case the ligand phen, reproduces a CV pattern very similar to that of the parent species.

The attribution, discussed above, of the processes as mainly centered on the different ligands for the various complexes is sketched in the diagram of Figure S1 (Supporting Information), where the reduction processes of the various complexes are related to each other as well as to those of the uncoordinated ligands.

In order to support the nature of the various electrochemical processes, quantum chemical calculations were undertaken at the DFT level for two of the most representative iridium complexes of the whole family, namely, $[Ir(thpy)_2(bpy)]^+$ and $[Ir(thpy\text{-}CHO)_2(bpy)]^+$. All of the calculations were carried out using the *Gaussian 03* program.[47] A preliminary screening of the most appropriate level of theory indicated that the best results were obtained at B3LYP/LanL2DZ,[48] which use a double-ζ quality basis set D95[49a] for the carbon, hydrogen, nitrogen,

(47) Frisch, M. J.; Trucks, G. W.; Schlegel, H. B.; Scuseria, G. E.; Robb, M. A.; Cheeseman, J. R.; Montgomery, J. A., Jr.; Vreven, T.; Kudin, K. N.; Burant, J. C.; Millam, J. M.; Iyengar, S. S.; Tomasi, J.; Barone, V.; Mennucci, B.; Cossi, M.; Scalmani, G.; Rega, N.; Petersson, G. A.; Nakatsuji, H.; Hada, M.; Ehara, M. Toyota, K. Fukuda, R.; Hasegawa, J.; Ishida, M.; Nakajima, T.; Honda, Y.; Kitao, O.; Nakai, H.; Klene, M.; Li, X.; Knox, J. E.; Hratchian, H. P.; Cross, J. B.; Bakken, V.; Adamo, C.; Jaramillo, J.; Gomperts, R.; Stratmann, R. E.; Yazyev, O.; Austin, A. J.; Cammi, R.; Pomelli, C.; Ochterski, J.; Ayala, P. Y.; Morokuma, K.; Voth, G. A.; Salvador, P.; Dannenberg, J. J.; Zakrzewski, V. G.; Dapprich, S.; Daniels, A. D.; Strain, M. C.; Farkas, O.; Malick, D. K.; Rabuck, A. D.; Raghavachari, K.; Foresman, J. B.; Ortiz, J. V.; Cui, Q.; Baboul, A. G.; Clifford, S.; Cioslowski, J.; Stefanov, B. B.; Liu, G.; Liashenko, A.; Piskorz, P.; Komaromi, I.; Martin, R. L.; Fox, D. J.; Keith, T.; Al-Laham, M. A.; Peng, C. Y.; Nanayakkara, A.; Challacombe, M.; Gill, P. M. W.; Johnson, B. G.; Chen, W.; Wong, M. W.; Gonzalez C.; Pople, J. A. *Gaussian 03*, revision C.02; Gaussian, Inc.: Wallingford, CT, **2004**.

(48) A combination of different functionals (BP86, B3LYP, and B3P86) and basis sets [i.e., (i) 6-31G* on carbon, hydrogen, nitrogen, and oxygen atoms and LanL2DZ ECP on sulfur and iridium atoms, (ii) 6-31G* on carbon, hydrogen, nitrogen, and oxygen atoms and SDD ECP on sulfur and iridium atoms, and (iii) LanL2DZ, i.e., D95, on carbon, hydrogen, nitrogen, and oxygen atoms and Los Alamos ECP plus DZ on sulfur and iridium atoms] has been used in the screening calculations. Geometry optimization using the combinations B3LYP/(6-31G*, LanL2DZ) and B3LYP/LanL2DZ gave very similar results and the lowest deviations of the bond lengths and bond angles from the X-ray values.

(49) (a) Dunning, T. H., Jr.; Hay, P. J. In *Modern Theoretical Chemistry*; Schaefer, H. F., III, Ed.;Plenum: New York, 1976; Vol. *3*, p 1.(b) Hay, P. J.; Wadt, W. R. *J. Chem. Phys.* **1985**, *82*, 299. (c) The ECP on the iridium replaced the inner-core electrons, leaving the outer-core $[(5s)^2(5p)^6]$ electrons and the $(5d)^6$ valence electrons of iridium(III).

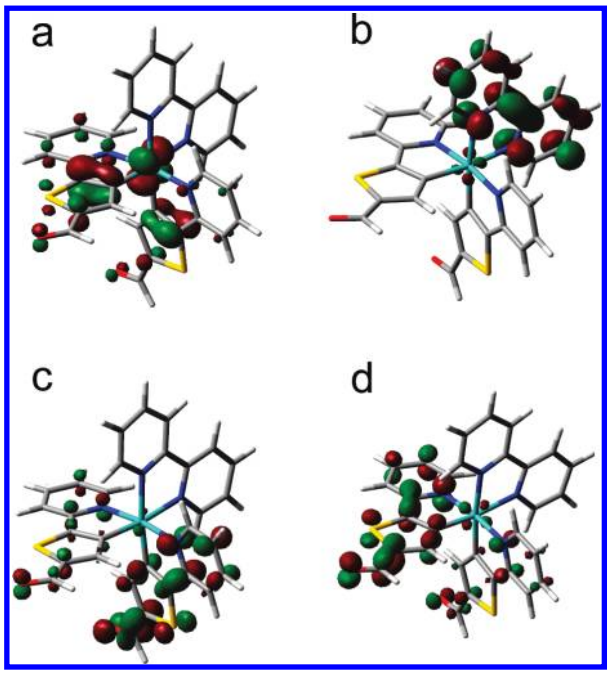

Figure 6. Plot of the frontier molecular orbital surfaces for the species $[Ir(thpy\text{-}CHO)_2(bpy)]^+$ showing the main localization of the orbitals involved in the redox processes: (a) HOMO (first oxidation) mainly centered on the iridium with a contribution from the thienyl moieties; (b) LUMO (first reduction) centered on bpy; (c and d) second and third unoccupied molecular orbitals (i.e., second and third reduction processes) centered on the two thpy ligands. Optimized geometries were at the B3LYP/LanL2DZ level of theory.

and oxygen atoms of the ligands and a relativistic effective core potential (ECP) for the iridium and sulfur atoms.[49b,c] Geometry optimization of the iridium complexes was carried out without any symmetry constraint, and the resulting calculated structures are in reasonably good agreement with the crystallographic data. The comparison of the calculated bond lengths for the optimized geometries with the X-ray data (vide supra) shows that the differences are, on average, within 0.03 Å.

For all of the species investigated, the plot of the highest occupied molecular orbital (HOMO) is centered on the metal with a substantial contribution from the thpy ligands, as is also reported for similar iridium cyclometalated complexes.[33] Conversely, the lowest unoccupied molecular orbital (LUMO) is mainly localized on the dipyridyl ligand. The two successive unoccupied molecular orbitals calculated for the pristine cationic complex $[Ir(thpy)_2(bpy)]^+$ (e.g., LUMO+1 and LUMO+2) have close energy values and are mainly localized on the two thpy ligands. Modeling of the reduced species $[Ir(thpy)_2(bpy)]^-$ and $[Ir(thpy)_2(bpy)]^{2-}$ indicates that the most stable electronic states are the triplet and quartet, respectively, which means that the first three electrons introduced are unpaired and mainly localized on the three ligands. Concerning the species $[Ir(thpy\text{-}CHO)_2(bpy)]^+$, the quantum chemical calculations, at the same level of theory, show a very similar molecular orbital sketch (Figure 6), with the difference that the unoccupied molecular orbitals localized on the thpy ligands have a lower energy because of the presence of the aldehydic groups.

This makes such ligands easier to reduce, as is also shown by the electrochemical results of the uncoordinated ligands (see Table 3), and, in turn, it also determines the occurrence of an electrochemically accessible second reduction on thpy-CHO when chelated to the metal center. Moreover, as far as the first three reductions are concerned, comparisons of the corresponding gas-phase theoretical results, for the two iridium species, are qualitatively in good agreement with the electrochemical findings (see Figure S2 in the Supporting Information).

Table 4. ECL Data for the Iridium Complexes Investigated in an ACN Solution at 25 °C

species	λ_{ECL} (nm)	Φ_{ECL} (%)[a]
$[Ir(thpy\text{-}CHO)_2bpy]^+$	642	0.5
$[Ir(thpy)_2bpy]^+$	608	0.4
$[Ir(thpy\text{-}CHO)_2dmbpy]^+$	635	0.3
$[Ir(thpy\text{-}CHO)_2phen]^+$	640	0.3
$[Ir(thpy\text{-}Me)_2bpy]^+$	630	0.1

[a] The ECL efficiency was calculated as reported in the Experimental Section.

ECL. The PL efficiency of the iridium complexes investigated in this work prompted us to consider these molecules as relatively good candidates for ECL studies.[17g] The ECL spectra of all of the species have been obtained in ACN by annihilation of the one-electron-oxidized and -reduced forms, and the data are collected in Table 4. The emission, although not very intense, shows a stable and reproducible behavior over a wide number of experiments performed with the same solution; thus, it is promising for a possible use in devices.

Concerning the energetics of the ECL process, on the basis of the emission wavelengths of the various compounds, the energy needed to generate the excited states, from which the emission takes place, ranges from 1.95 eV for $[Ir(thpy\text{-}CHO)_2dmbpy]^+$ to 2.03 eV for $[Ir(thpy)_2bpy]^+$. As in a typical annihilation ECL experiment, the energy to generate the emitting excited state is provided by the homogeneous electrochemical reaction between the electrochemically generated oxidized and reduced species; the energy requirements above must be fulfilled by the electrochemical data. Thus, the annihilation reaction enthalpy, $\Delta H^\circ_{ann} = \Delta G^\circ_{ann} + T\Delta S^\circ$, must be high enough to generate the emitting state. ΔG°_{ann} is obtained from the half-wave potential difference between the first oxidation and first reduction waves in the cyclic voltammogram [$\Delta E_{1/2}$(ox/red)], which is comprised of, for the compounds investigated here, between 2.3 and 2.6 V. If we consider an entropy contribution ≈0.1 eV,[35,36,17b] we obtain a minimum value of 2.2 eV for ΔH°_{ann}, which is, for all of the species, higher than the minimum energy required for the population of the excited state (estimated from the emission spectra, vide supra).

The ECL experiments were carried out by pulsing the potential between the first oxidation and first reduction processes by both cyclic voltammetry and double-step potential techniques. The ECL spectra recorded in dry ACN for the species $[Ir(thpy\text{-}CHO)_2bpy]^+$, $[Ir(thpy\text{-}CHO)_2phen]^+$, and $[Ir(thpy)_2bpy]^+$ are shown in Figure 7a−c, respectively, and no differences in the ECL signals were observed when the potential window was extended in the reduction to include the second process. Concerning the mechanism of the excited-state generation, further studies are currently underway, and we can only speculate that, most

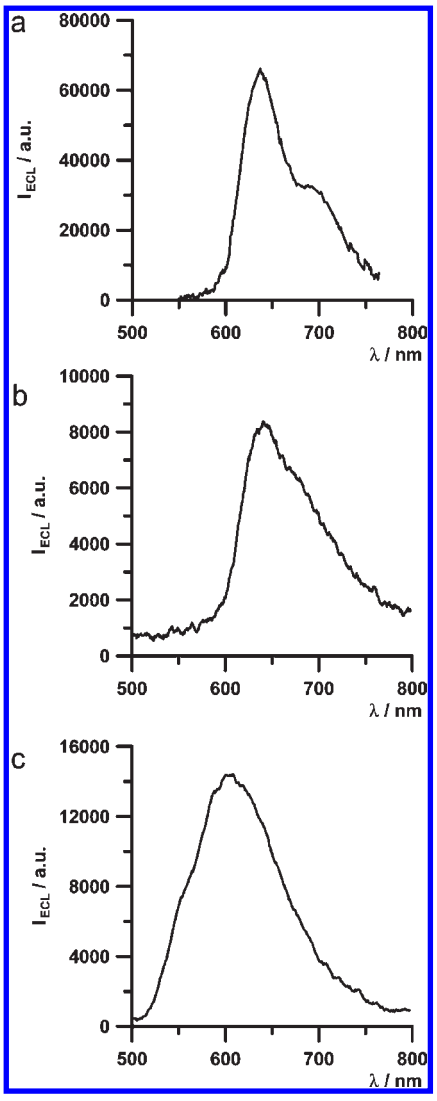

Figure 7. ECL spectra of the (a) $[Ir(thpy\text{-}CHO)_2bpy]^+$, (b) $[Ir(thpy\text{-}CHO)_2phen]^+$, and (c) $[Ir(thpy)_2bpy]^+$ obtained by annihilation of one-electron-oxidized and -reduced forms. All ECL spectra were collected for a 1 mM compound in a 0.07 M TBAH/ACN electrolyte solution, at 25 °C.

likely, the main annihilation path does involve the direct formation of the triplet state.

The ECL spectra of the iridium compounds investigated are characterized by broad emission bands comprised of between 520 and 750 nm. The maxima were between 600 and 650 nm. When compared to the luminescence, the ECL spectra show some differences (see Figure S3 in the Supporting Information), being slightly broader in shape, with λ_{max} at about the same value or eventually shifted to lower energy (by $\leq$10 nm for $[Ir(thpy\text{-}CHO)_2bpy]^+$). This difference is probably due to the lower resolution of the ECL instrument where the spectra were collected. This is also the reason why for some iridium complexes the vibronic structure is less evidenced in the ECL spectra than in the PL one. Anyway, information relative to the vibronic structure can still be extracted from the experimental spectra, as shown in Figures S4 and S5 in the Supporting Information.

It is sometimes reported that the observed ECL band is significantly shifted at a longer wavelength region as compared to the PL spectrum, and this might be due to (i) the formation of side products generated during the annihilation or (ii) the formation of excited-state aggregates, at the concentration used to obtain the spectrum. Because no change in the absorption and PL spectra was observed before and after extensive potential cycling, this suggests that in the case of $[Ir(thpy\text{-}CHO)_2bpy]^+$ the second hypothesis holds (e.g., the formation of excited-state aggregates must be invoked).

ECL yields were determined using $[Ru(bpy)_3]^{2+}$ as a standard by comparison of the measured integrated photon intensities, taking into account the differences in the electric charges passed through the solution studied. The ECL efficiency (in photons emitted/electron transferred between reduced and oxidized forms of the parent molecule) is related directly to the yield of the excited state upon annihilation (Φ_{es}) and to the emission quantum yield (Φ_0) of a given emitter ($\Phi_{ECL} = \Phi_{es}\Phi_0$). The results obtained imply that the yield for the formation of the excited state is about 30−40%, which would make these systems promising for consideration in future development.

Conclusions

In this paper, a new class of air-stable cationic-functionalized bipyridyl-cyclometalated iridium(III) complexes, with thienyl-based ligands, have been synthesized and thoroughly characterized by studying their crystallographic, spectroscopic, luminescence, and electrochemical properties. The aldehydic functionality on the cyclometalated ligands makes these iridium complexes particularly interesting for further functionalization of reductive amination reactions. The electrochemical investigation showed a rich pattern of reduction processes that have been successfully attributed through a combined comparison of the CV behaviors of the iridium species and the free ligands. The various complexes are luminescent, with efficiency lower than that of similar cyclometalated phenylpyridine-based iridium(III) species but within the same range as that of previously reported thienyl-containing iridium(III) compounds. Interestingly, the complexes with the formyl-functionalized thienyl ligands have the highest luminescence efficiency of the series. Moreover, the ECL results show a trend very similar to that of the luminescence ones, featuring, in some cases, a relatively good ECL efficiency, which makes such systems potentially interesting in the field of new materials for electrochemiluminescent biodetection or polymeric light-emitting devices.

Acknowledgment. Acknowledgment is made to the Ministero dell'Istruzione, Università e Ricerca, MIUR, FIRB Project (Progettazione, preparazione e valutazione biologica e farmacologica di nuove molecole organiche quali potenziali farmaci innovativi), University of Bologna, and LATEMAR (centre of excellence financed by MIUR). INSTM and CINECA are also acknowledged for a computing time grant for use of the IBM SP5 mainframe. This paper is dedicated to Prof. Saverio Florio in occasion of his 70th birthday.

Supporting Information Available: Crystallographic data table of $[Ir(thpy)_2bpy]PF_6$, $[Ir(thpy\text{-}CHO)_2bpy]PF_6$, and $[Ir(thpy\text{-}CHO)_2phen]PF_6$, DFT-calculated energies and molecular orbital compositions, diagram of the reduction processes of the iridium complexes and the uncoordinated ligands, and Gaussian deconvolution of the PL and ECL spectra of the species $[Ir(thpy\text{-}CHO)_2phen]^+$ and $[Ir(thpy)_2bpy]^+$ in ACN. This material is available free of charge via the Internet at http://pubs.acs.org.